GSA DATA REPOSITORY 2014285

Carbon-forming reactions under a reducing atmosphere during seismic fault slip

Kiyokazu Oohashi*, Raehee Han, Takehiro Hirose, Toshihiko Shimamoto,
Kentaro Omura, and Tatsuo Matsuda
*Corresponding author, E-mail address: oohashik@earth.s.chiba-u.ac.jp

Contents

1. Details of the Experimental Apparatus and Procedures

We conducted high-velocity friction experiments using a rotary-shear, low- to high-velocity friction apparatus at Hiroshima University (HDR apparatus; Togo and Shimamoto, 2012) and a high-velocity friction apparatus at Kochi Institute for Core Sample Research/JAMSTEC (HVR apparatus; Shimamoto and Tsutsumi, 1994; Hirose and Shimamoto, 2005). Both apparatuses were equipped with a small specimen chamber/vessel to contain a gas around the sample (Fig. DR1). For the HDR apparatus, rubber O-rings were placed at the top and bottom of the acrylic chamber to prevent gas leakage and inflow of air. Before the experiments, we evacuated the chamber and recharged it with N_2 gas three times, and then charged it with a selected gas (N_2 or H_2). We confirmed that the relative humidity in the vessel was less than 2%, the detection limit of the sensor, during the experiments. The measured torque supported by the O-rings was less than 0.05 Nm, corresponding to a shear stress of ~0.01 MPa. For the experiments with the HVR apparatus, the O-ring was removed from the pressure vessel to detect emitted CH_4 gas from the sliding surface, because CH_4 gas was also released from the dynamic O-ring as a result of abrasion during experiments. Therefore, CH_4 gas (as well as the other gases) diffused from the vessel into the chamber, meaning that we

were unable to determine the concentration of gas accurately in this study. However, we were able to examine whether CH_4 gas was generated from the sliding surface during shearing. We also sealed the specimen chamber in which the vessel and holder were placed (Fig DR1B) with an acrylic plate to keep the anoxic atmosphere around specimens during the experiments. We flowed N_2 gas through the vessel (and the chamber) for five minutes to remove air, and then charged the vessel with N_2 or H_2 gas before a run. The sealing of the acrylic plate was sufficient to constrain O_2 concentration in the vessel and chamber to less than 2% both before and during the experiment.

Because the slip rate increases from the center to the periphery of the cylindrical specimens, we used the equivalent slip rate, V_e, defined such that $\tau V_e S$ gives the rate of total frictional work on a fault with area S, assuming a constant shear stress τ over the fault surface (Shimamoto and Tsutsumi, 1994). For convenience, we refer to "equivalent slip rate" as simply "slip rate" or "velocity" in the main text.

Figure DR1. A: Photograph of the acrylic chamber and specimen holder of the HDR apparatus. The lower specimen is moved up to contact the simulated fault surface and then the chamber is pulled down to supply gas around the specimens. B: Photograph of the metal pressure vessel and specimen holder of the HVR apparatus, with diagrams showing the gas supply system and a gas chromatograph (see also figure S2 in Hirose et al., 2011). The vessel and holder were placed in the specimen chamber, which was also sealed with an acrylic plate (see appendix 1 in Sato et al., 2009).

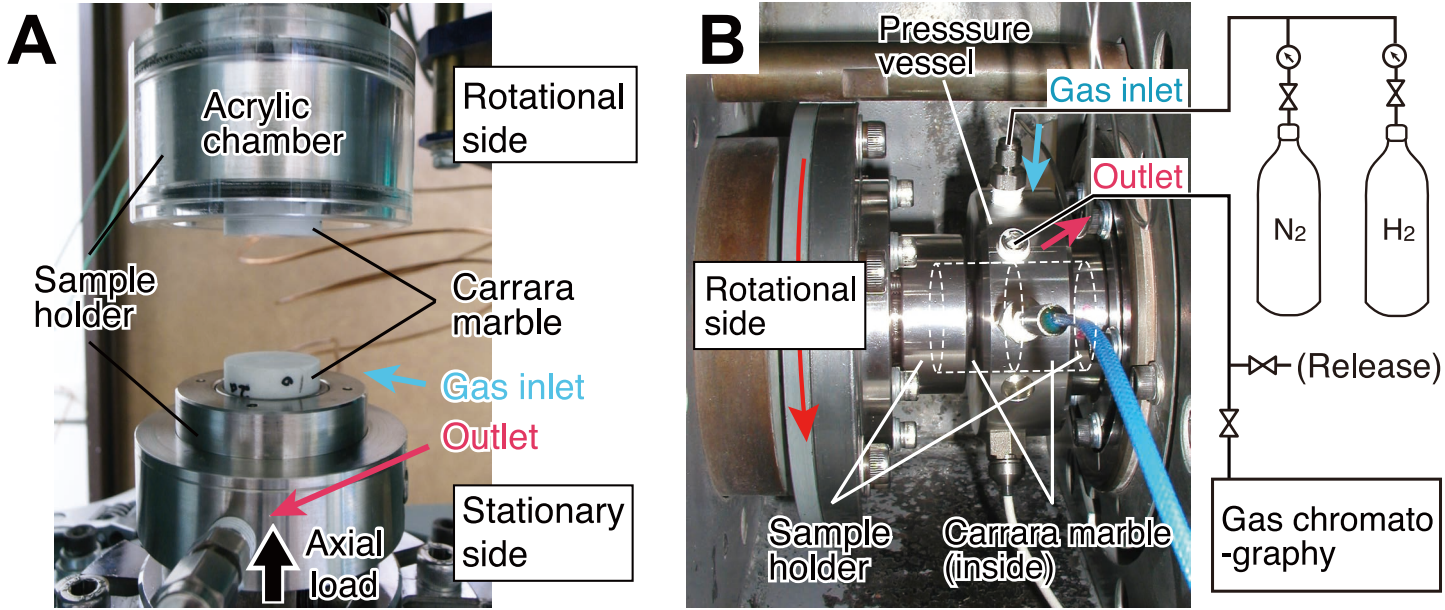
A
Acrylic chamber
Rotational side
Sample holder
Carrara marble
Gas inlet
Outlet
Stationary side
Axial load
B
Presssure vessel
Gas inlet
Outlet
Rotational side
Sample holder
Carrara marble (inside)
N2
H2
(Release)
Gas chromato -graphy

Figure DR1

2. Details of the Peak Decomposition Methods of Raman Spectra

We conducted peak decomposition of observed Raman spectra using the commercial software Igor Pro 6.22 (WaveMetrics Inc.) with Gaussian and Lorentzian functions. Because the spectra of the blackish gouge show characteristics of low-grade (amorphous-like) CM rather than those of high-grade (crystallized) CM, we used the peak decomposition method proposed by Kouketsu et al. (2013) for analyzing low-grade CM and obtained the results shown in the lower part of Figure 3B. Before the peak decomposition, the spectrum was corrected for the fluorescence background by subtracting a linear baseline in the spectral range of 900–1900 cm^{-1}. The Raman spectra of intermediate- to high-grade CM usually contain G (graphite) band at ~1580 cm^{-1}, associated with the $E_{2\,g2}$ vibration mode of ideal graphitic lattice. However, the peak at around 1600 cm^{-1} could not be separated into D2 and G bands in all cases, and the latter is vanishingly small if it even exists. We therefore treat the peak at around 1600 cm^{-1} as a single peak (D2 band) in the present study.

3. Supplementary Data

Table DR1. Summary of experimental data reported in this paper. HDR or HVR in run numbers refers to the apparatus used in experiments. Slip-weakening parameters were determined for slip-weakening parts of the friction-displacement curves without including the data for subsequent slip strengthening, and hence μ_{ss} values in some runs are not strictly the steady-state friction coefficient. Gas concentration is shown only for CO_2, H_2, and CH_4. Symbols μ_p: peak friction coefficient; μ_{ss}: steady-state friction coefficient; D_c: slip-weakening displacement; SE: standard error. The μ_{ss} values in brackets denote temporal steady-state friction before strengthening.

Table DR1

Experiment number	Atmosp-here	Normal stress (MPa)	Displace-ment (m)	Duration (s)	μ_p	μ_{ss}		D_c (m)		Gas chromatographic analysis (ppm)			Formation of blackish material
						Average	SE	Average	SE	CO_2	H_2	CH_4	
HDR641	H_2	2.0	59.8	46.0	0.59	0.12	0.00	32.5	0.24				common
HDR642	H_2	2.4	97.9	75.3	0.77	(0.09)	0.00	3.9	0.03				little
HDR677	H_2	3.0	105.5	81.1	0.31	(0.03)	0.00	6.6	0.09				little
HDR678	H_2	2.4	79.4	61.1	0.82	(0.12)	0.00	4.4	0.07				common
HDR679	H_2	3.1	71.5	92.8	0.37	(0.11)	0.00	2.2	0.03				none
HVR2590	H_2	3.1	49.5	39.5	0.74	0.03	0.00	18.6	0.20	687	7197	none	common
HVR2591	H_2	3.1	49.8	38.3	0.61	0.06	0.00	26.8	0.13	65666	3921	133	little
HVR2593	H_2	3.1	60.1	46.7	0.75	0.08	0.00	15.5	0.08	634	53190	none	common
HDR676	N_2	3.0	94.0	72.3	0.25	0.11	0.00	7.4	0.23				none
HVR2592	N_2	3.1	87.3	67.1	0.76	0.15	0.00	1.4	0.04				none
HDR675	Air	3.0	50.3	38.7	0.89	0.08	0.00	37.1	0.43				none

References

Hirose, T., Kawagucci, S., and Suzuki, K., 2011, Mechanoradical H_2 generation during simulated faulting: Implications for an earthquake-driven subsurface biosphere: Geophysical Research Letters, 38, L17303, doi:10.1029/2011GL048850.

Hirose, T., and Shimamoto, T., 2005, Growth of molten zone as a mechanism of slip weakening of simulated faults in gabbro during frictional melting: Journal of Geophysical Research, 110, B05202, doi:10.1029/2004JB003207.

Kouketsu, Y., Mizukami, T., Mori, H., Endo, S., Aoya, M., Hara, H., Nakamura, D., and Wallis, S., 2013, A new approach to develop the Raman carbonaceous material geothermometer for low-grade metamorphism using peak width: The Island Arc, doi:10.1111/iar.12057.

Sato, K., Kumagai, H., Hirose, T., Tamura, H., Mizoguchi, K., Shimamoto, T., 2009, Experimental study for noble gas release and exchange under high-speed frictional melting: Chemical Geology, 266, p. 96–103 doi:10.1016/j.chemgeo.2008.12.017.

Shimamoto, T., and Tsutsumi, A., 1994, A new rotary-shear high-velocity friction testing machine: Its basic design and scope of research: Structural Geology, 39, p. 65–78 (in Japanese with English abstract).

Togo, T., and Shimamoto, T., 2012, Energy partition for grain crushing in quartz gouge during subseismic to seismic fault motion: an experimental study: Journal of Structural Geology, 38, 139–155.